



Contents lists available at SciVerse ScienceDirect

Bioorganic & Medicinal Chemistry Letters

journal homepage: www.elsevier.com/locate/bmcl

Novel adenosine A_{2A} receptor ligands: A synthetic, functional and computational investigation of selected literature adenosine A_{2A} receptor antagonists for extending into extracellular space

Manuela Jörg^a, Jeremy Shonberg^a, Frankie S. Mak^b, Neil D. Miller^b, Elizabeth Yuriev^a, Peter J. Scammells^{a,*}, Ben Capuano^{a,*}

^a Medicinal Chemistry, Monash Institute of Pharmaceutical Sciences, 381 Royal Parade, Parkville, Victoria 3052, Australia

^b GlaxoSmithKline, GSK R&D China, Singapore Research Centre, 11 Biopolis Way, Helios Bldg #03-01/02, Singapore 138667, Singapore

ARTICLE INFO

Article history:

Received 18 January 2013

Revised 15 March 2013

Accepted 20 March 2013

Available online xxx

Keywords:

Parkinson's disease

Adenosine A_{2A} antagonist

ZM 241385

KW 6002

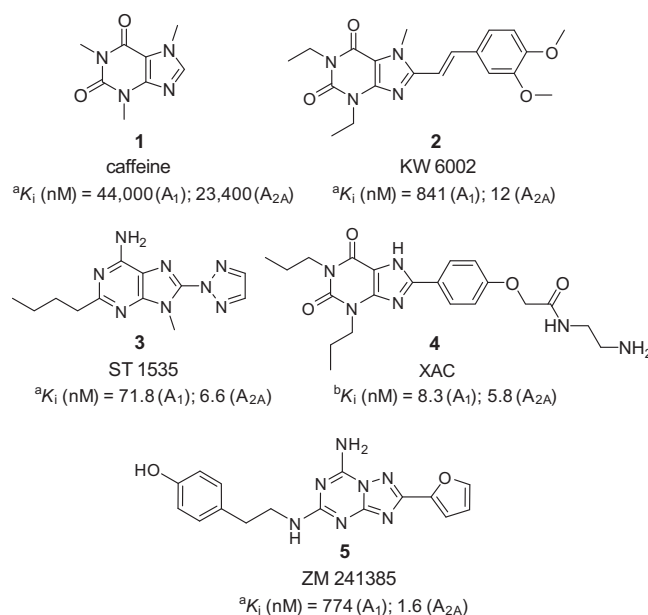
Congener

ABSTRACT

Growing evidence has suggested a role in targeting the adenosine A_{2A} receptor for the treatment of Parkinson's disease. The literature compounds KW 6002 (**2**) and ZM 241385 (**5**) were used as a starting point from which a series of novel ligands targeting the adenosine A_{2A} receptor were synthesized and tested in a recombinant human adenosine A_{2A} receptor functional assay. In order to further explore these molecules, we investigated the biological effects of assorted linkers attached to different positions on selected adenosine A_{2A} receptor antagonists, and assessed their potential binding modes using molecular docking studies. The results suggest that linking from the phenolic oxygen of selected adenosine A_{2A} receptor antagonists is relatively well tolerated due to the extension towards extracellular space, and leads to the potential of attaching further functionality from this position.

Crown Copyright © 2013 Published by Elsevier Ltd. All rights reserved.

Adenosine initiates most of its physiological effects through the activation of four G protein-coupled receptor (GPCR) subtypes; A₁, A_{2A}, A_{2B}, and A₃.^{1,2} These four receptor subtypes play an important role in the regulation of a number of central nervous system functions, including pain, cerebral blood flow, basal ganglia operation, respiration, and sleep.³ The receptors primarily operate by coupling to the cyclic adenosine monophosphate (cAMP) second-messenger system, and the adenosine A_{2A} receptor (A_{2A}R) in particular is linked to G_s and G_{o1f} proteins. Upon A_{2A}R activation, the intracellular levels of cAMP are increased.³ Interestingly, it was found that consuming just one cup of coffee per day reduces the incidence of Parkinson's disease by as much as five-fold;⁴ postulated to result from the antagonism of the A_{2A}R by caffeine (**1**) (Fig. 1).⁵ Furthermore, co-administration of KW 6002 (**2**) (Fig. 1) with the dopamine D₂ receptor agonist apomorphine has been shown to prevent the adverse effect of dyskinesias observed in monotherapy.⁶ Similar results were observed in rats when using the A_{2A}R antagonist ST 1535 (**3**) (Fig. 1) in combination with levodopa.⁷ Therefore, it is postulated that caffeine (**1**) and other A_{2A}R antagonists have potential as



* Corresponding authors. Tel.: +61 3 9903 9542 (P.J.S.); tel.: +61 3 9903 9556 (B.C.).

E-mail addresses: peter.scammells@monash.edu (P.J. Scammells), ben.capuano@monash.edu (B. Capuano).

0960-894X/\$ - see front matter Crown Copyright © 2013 Published by Elsevier Ltd. All rights reserved.
<http://dx.doi.org/10.1016/j.bmcl.2013.03.070>

Figure 1. Chemical structures of some important adenosine receptor antagonists and their respective K_i values at the human A₁ and A_{2A} receptor in nM. (a) Data from (cAMP) studies (Müller and Jacobson, 2011);¹¹ (b) Data from (cAMP) studies (Kecskés et al., 2011).¹²

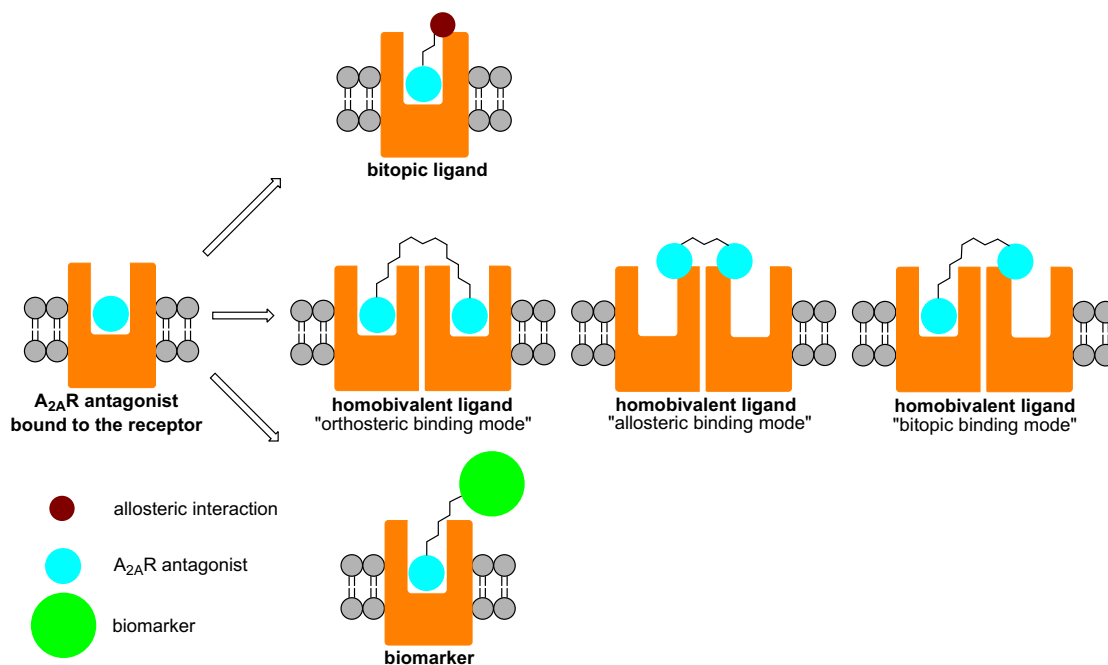
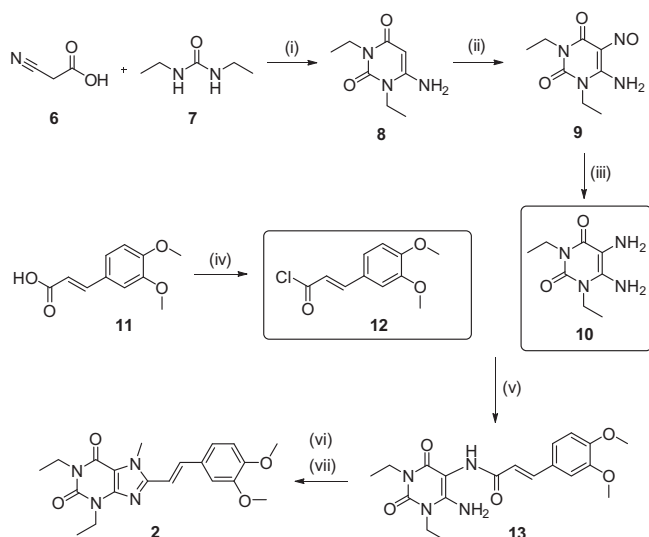


Figure 2. A schematic example of possible binding modes for probes incorporating an $A_{2A}R$ antagonist: bitopic ligand (upper), homobivalent ligand and hypothetical binding modes (middle) and biomarker (lower).

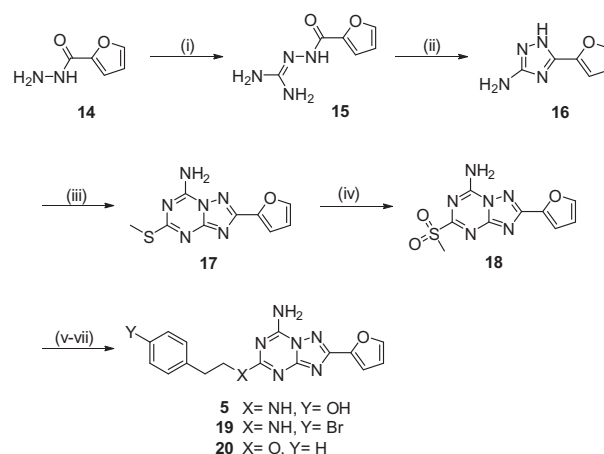
neuroprotective agents against neuronal degeneration observed in Parkinson's disease.^{8–10}

A strategy in drug discovery programs with increasing popularity is the concept of hybrid molecules targeting GPCRs,^{13–15} whereby single molecular entities target multiple binding sites on one receptor (bitopic ligand), or adjacent receptors (hetero- or homobivalent ligand) simultaneously (Fig. 2). In the second case, multiple binding modes have to be considered; both pharmacophores possibly bind to an orthosteric or allosteric site or the hetero-/homobivalent ligand could interact in a bitopic mode across two dimers, that is one pharmacophore binds to the orthosteric site of receptor 1 and the second pharmacophore binds to an

allosteric site on receptor 2 (Fig. 2, middle). Ligands of that type offer potential advantages such as enhanced potency and receptor subtype selectivity and improved pharmacokinetics compared to a multi-drug regimen.^{13,16–18} Furthermore, significant research has focused on the design of biomarkers and fluorescent ligands targeting the adenosine receptors in an effort to further characterize their role in important disease states (Fig. 2).^{19,20} For all of these novel concepts, the ligand must allow for extension towards the extracellular space from the original binding mode to avoid any significant loss of biological activity. A well-established example of this concept is the high affinity xanthine amine congener, XAC (4) (Fig. 1).^{11,21} The relatively insensitive amine terminal of XAC



Scheme 1. Synthesis of KW 6002 (**2**). Reagents and conditions: (i) acetic anhydride, 80 °C, 2 h, 83%; (ii) sodium nitrite, 50% acetic acid, 60 °C, 15 min, 86%; (iii) sodium dithionite, NH_4OH solution (12.5% (w/v)), 60 °C, 30 min, 98%; (iv) $SOCl_2$, toluene, 75 °C, 2 h, 97%; (v) pyridine, DCM, rt, 16 h, 66%; (vi) HMDS, cat. $(NH_4)_2SO_4$, CH_3CN , 160 °C, microwave, 5 h, 100% followed by (vii) MeI, K_2CO_3 , DMF, rt, 2 h, 75%.



Scheme 2. Synthesis of ZM 241,385 (**5**) and analogs **19** and **20**. Reagents and conditions: (i) (*S*)-methylisothiosulfate hemisulfate, NaOH, water, rt, 24 h, 58%; (ii) water, microwave, 140 °C, 1 h, 99% or water, reflux, 29 h, 80%; (iii) *N*-cyanodithioiminocarbonate, 170 °C, 1 h, 32%; (iv) *m*-CPBA, DCM, 22 h, 83%; (v) tyramine, CH_3CN , rt, 22 h, 33% (**5**); (vi) 4-bromophenethylamine, CH_3CN , rt, 18 h, 32% (**19**); (vii) 2-phenethyl alcohol, DBU, DME, reflux, 1 h, 20% (**20**).

(4) has been used for extending into the extracellular space with multi-functionalized molecules targeting adenosine receptors.^{21,22}

This study has focused on identifying the ideal position to attach linkers to known and novel structurally related A_{2A}R antagonists in order to extend into extracellular space with minimal penalty on binding affinity; thus allowing potential attachment of further functionalities. The literature A_{2A}R antagonists, KW 6002 (**2**) and ZM 241,385 (**5**) (Fig. 1), served as lead compounds to design novel molecules, as well as, to monitor the effects of various linker types and lengths.

The synthesis of KW 6002 (**2**) (Scheme 1) consisted of a convergent pathway from two starting points; namely the synthesis of the diaminouacil (**10**) following a procedure by Hockemeyer et al.,²³ and the preparation of the acid chloride **12**. Subsequent reaction of **10** and **12** afforded the intermediate scaffold **13**.²³ Ring closure was performed in a microwave reactor in the presence of hexamethyldisilazane and catalytic ammonium sulfate following a modified procedure by Burbiel et al.²⁴ to obtain the xanthine motif. Extended reaction time of 5 h was required to promote reaction completion in quantitative yield. Finally, N-methylation of the xanthine with iodomethane and potassium carbonate afforded KW 6002 (**2**) in good yield.

ZM 241,385 (**5**) is a potent and selective A_{2A}R antagonist^{25,26} and the first ligand for which crystal structures in complex with the A_{2A}R have been solved.^{3,27} ZM 241,385 (**5**) was synthesized according to Scheme 2.²⁸ The synthetic pathway has been adapted from the original patent where the A_{2A}R antagonist **5** was manufactured from aminoguanidine nitrate and 2-furonitrile.²⁵ Our reaction pathway commenced with commercially available 2-furanhydrazide (**14**) and incorporates fairly inexpensive reagents. The conditions used to afford intermediates **15**²⁹ and **16**³⁰ have been previously published but not in context with the preparation of ZM 241,385 (**5**). The final three steps were performed following a patent procedure described by Caulkett et al.²⁵ The overall yield for the synthetic pathways illustrated in Scheme 2 was 5% (>97% purity by analytical HPLC, 214 nm and 254 nm).²⁸ Compounds **19** and **20** were synthesized using the same general synthetic pathway. A non-nucleophilic base (1,8-diazabicycloundec-7-ene) was employed in the final step of the synthesis of compound **20** for reaction progression.²⁵

We designed and synthesized three novel hybrid compounds **21–23** based on the structures of ST 1535 (**3**)³¹ and ZM 241,385 (**5**)²⁵ (Fig. 3). The hypothesis was that these novel compounds

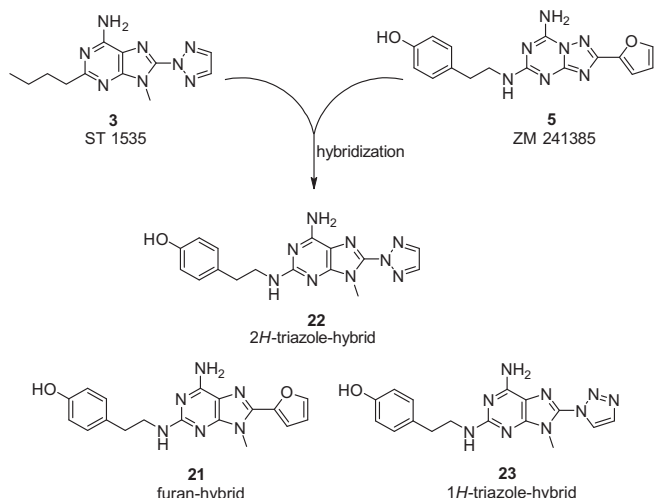
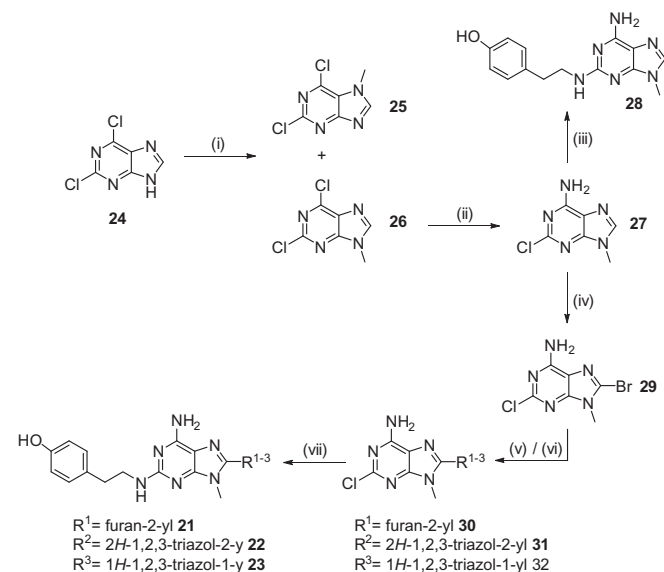


Figure 3. Overview of the novel hybrids **21–23** derived from the parent compounds ST 1535 (**3**) and ZM 241,385 (**5**).



Scheme 3. Synthesis of the furan-hybrid **21**, the triazole-hybrids **22** and **23** and model compound **28**. Reagents and conditions: (i) MeI, K₂CO₃, CH₃CN, rt, 24 h, 1:4 (**25**:**26**), 48% (**26**); (ii) NH₄OH solution (32% (w/v)), CH₃CN, 55 °C, 25 h, 82%; (iii) tyramine, DIPEA, DMSO, 145 °C, 42 h, 32%; (iv) bromine, THF/MeOH/sodium acetate buffer pH 4 1:1:1, –10 °C, 10 min then rt, 20 min, 60%; (v) 2-furanboronic acid, Pd(PPh₃)₄, Cs₂CO₃, DME/water 10:3, 85 °C, 20 h, 51% (**30**); (vi) 1*H*-1,2,3-triazole, Cs₂CO₃, DMF, 80 °C, 20 h, 32% (**31**) and an enriched mixture of **31** and **32**; (vii) tyramine, DIPEA, DMSO, 145 °C, 42 h, 32% (**21**); 28 h, 32% (**22**); 28 h, 10% (**23**).

may have comparable activity as A_{2A}R antagonists due to their structural and functional similarities. The furan-hybrid **21** differs from ZM 241,385 (**5**) only by the replacement of the nitrogen atom in position 5 with a carbon atom (diazolodiazine or purine), and has a methyl group at position 7. The 2*H*-triazole-hybrid **22**, on the other hand, is very similar to the structure of ST 1535 (**3**) except the alkyl chain is substituted with a tyramine moiety.

Hybrids **21–23** were synthesized via a five step pathway starting from commercially available 2,6-dichloropurine (**24**) (Scheme 3). The methyl group was successfully introduced under alkaline conditions using methyl iodide in acetonitrile.³² The ratio of the isomers **25** and **26** according to the crude ¹H NMR was about 1:4 favouring the desired product **26**. The isomers **25** and **26** were separable by column chromatography. The amination of compound **26** at position 6 (resulting from the nucleophilic substitution of Cl) was performed in 32% ammonia solution at room temperature.³³ The crude material was purified by suspending it in methanol followed by filtration; resulting in an excellent yield (82%). The reaction was also performed using 2*N* ammonia solution in methanol but these reaction conditions gave a complex mixture of the desired product **27** and a by-product where the chlorine at position 6 was substituted with a methoxy group. The substitution of the chlorine in position 5 with tyramine (**28**) was investigated as a model reaction for target compounds **21–23**. In this reaction, tyramine was attached to **27** under alkaline conditions at 145 °C. Product **28** was obtained in a reasonable yield of 32%. Subsequent bromination of **27** using neat bromine at room temperature in a solvent mixture of tetrahydrofuran/methanol/sodium acetate buffer (pH 4)³⁴ afforded, after purification by column chromatography, product **29** (60% yield). Despite optimization (longer reaction time, heating to 50 °C and different solvent systems), 10–20% of starting material failed to convert into the desired product **29**. Attempts to effect this transformation using *N*-bromosuccinimide and *N*-iodosuccinimide were unsuccessful. In the case of the furan-hybrid **21**, the intermediate **29** was further reacted under Suzuki coupling conditions with 2-furanboronic acid to give

the desired product **30** in 51% yield. The final step towards the synthesis of **21** was the nucleophilic aromatic substitution of chlorine with tyramine, which employed the model alkaline conditions at 145 °C used for the preparation of **28**. The furan-hybrid **21** was isolated as a white solid in 30% yield and, following column chromatography and recrystallization, was obtained with purity greater than >95% (analytical HPLC, 214 nm and 254 nm). To furnish the triazole-hybrids **22** and **23**, compound **29** was initially reacted with 1*H*-1,2,3-triazole.³⁵ This reaction was performed under alkaline conditions in *N,N*-dimethylformamide at 80 °C. After 20 h, all the starting material was converted to products **31** and **32**, which could not be separated by column chromatography. Nevertheless, we obtained isomer **31** with >91% purity (analytical HPLC, 214 nm and 254 nm), which was subsequently added to tyramine to obtain the desired 2*H*-triazole-hybrid **22** in 32% yield. Tyramine was combined with the mixture of intermediates **31** and **32** as a means of retrospectively characterizing compound **32** through the structural elucidation of **23**. This reaction gave the expected mixture of compounds **22** and **23**, and after column chromatography and recrystallization, a sample of compound **23** (>95% purity by analytical HPLC, 214 nm and 254 nm) was obtained in 10% yield.

This study focused on the identification of the optimal position to attach a linker for extending towards the extracellular space with minimal penalty on binding potency. The design of such compounds was aided by published crystal structures of the A_{2A}R with bound antagonists XAC (**4**) (3REY, cyan)²⁷ and ZM 241,385 (**5**) (3EML, green).³ The crystal structures show the binding mode of the nitrogen-rich aromatic heterocycle deep into the binding cavity (Fig. 4), thus allowing the *para*-substituted phenolic portion to extend towards extracellular space. In order to further explore this binding mode, we synthesized ligands with linker attachment in various positions, and assessed their inhibitory potency at the A_{2A}R.

The antagonist KW 6002 (**2**) shares structural similarity with XAC (**4**). KW 6002 analog **41** and **42**, with linkers attached through the *para*-methoxy position of KW 6002 (**2**), were synthesized according to Scheme 4. The key intermediate **38** was synthesized using the same procedure as illustrated in Scheme 1 for the synthesis of KW 6002 (**2**). However, to achieve a single point for attach-

ment of the linker portion, the synthesis commenced with ferulic acid (**33**), with the phenol first protected as the acetate in acetic anhydride and pyridine, to give **34**. Acyl chloride formation, amide coupling and ring closure occurred under the same conditions as shown in Scheme 1, with the concomitant loss of the acetyl group, to give xanthine **37**. Regioselective *N*-methylation of **37** was achieved with lithium bis(trimethylsilyl)amide and slow addition of iodomethane to give **38** in good yield. The phenol group was alkylated with ethyl 4-bromobutyrate (**39**), to give ether linked functionality to the molecule. Further elaboration was accomplished by ethyl ester deprotection of **39** in sodium hydroxide and methanol with acidic workup to furnish the carboxylic acid **40**, followed by BOP-mediated amide coupling to give **41** and **42**.

To produce ZM 241,385 analogs, we initially investigated the phenolic oxygen of ZM 241,385 (**5**) for forming an ether linkage (Scheme 5). Compound **5** was combined with ethyl 4-bromobutyrate under alkaline conditions, but the synthesis was insufficiently selective and resulted in a mixture of **43–45**, which were separated chromatographically. The formation of an ether linkage via Mitsunobu reaction conditions also failed. A synthetic route to selectively obtain **43** has been subsequently discovered, which entails *O*-alkylation of Boc-protected tyramine with ethyl 4-bromobutyrate, followed by removal of the protecting group to reveal the primary amine, and finally nucleophilic substitution of the sulfone intermediate **18**. Next, we investigated the formation of an ester linkage under acidic conditions whereby three linkers of various lengths were attached to ZM 241,385 (**5**) (Scheme 6). This protocol proved to be productive as the acidic conditions circumvented the formation of the previously observed *N*-substituted by-products (Scheme 5).

These linker types (ether and ester linkage) were also attached to the structurally related 2*H*-triazole-hybrid **22**, as illustrated in Scheme 7. Unlike for ZM 241,385 (**5**), alkylation and acylation afforded the desired *O*-linked product selectively.

To identify A_{2A}R specific antagonists, we utilized a recombinant cell-based cAMP competitive immunoassay, the LANCE™ cAMP Kit from PerkinElmer. The assay was used to compare the activity (IC₅₀) of the potentially novel A_{2A}R antagonists with the literature compounds as well as to determine the most suitable attachment position of the linker (Table 1). The comparison of the pIC₅₀ values

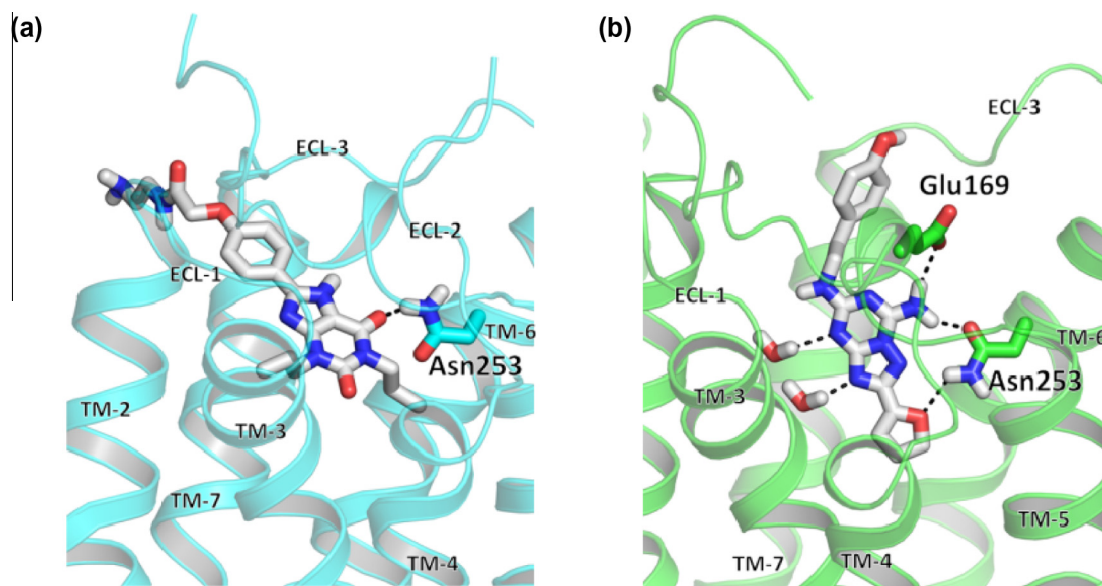
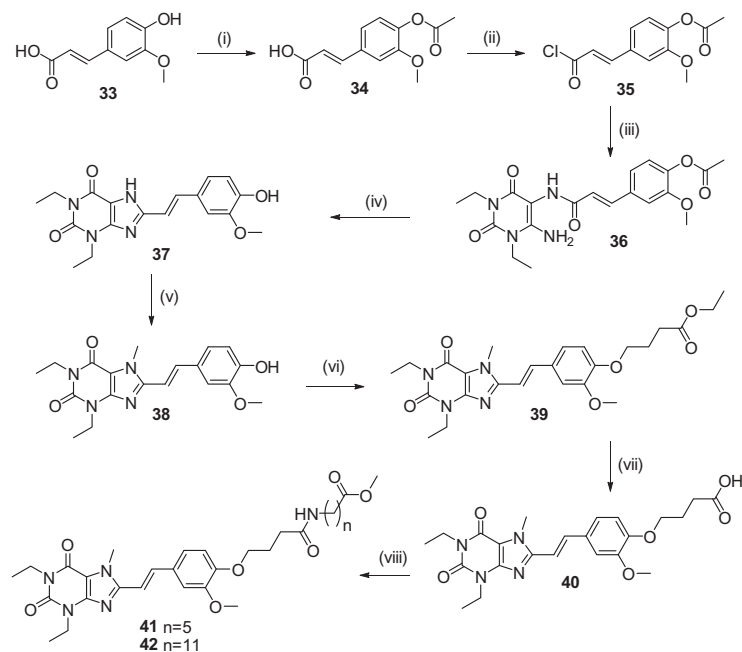
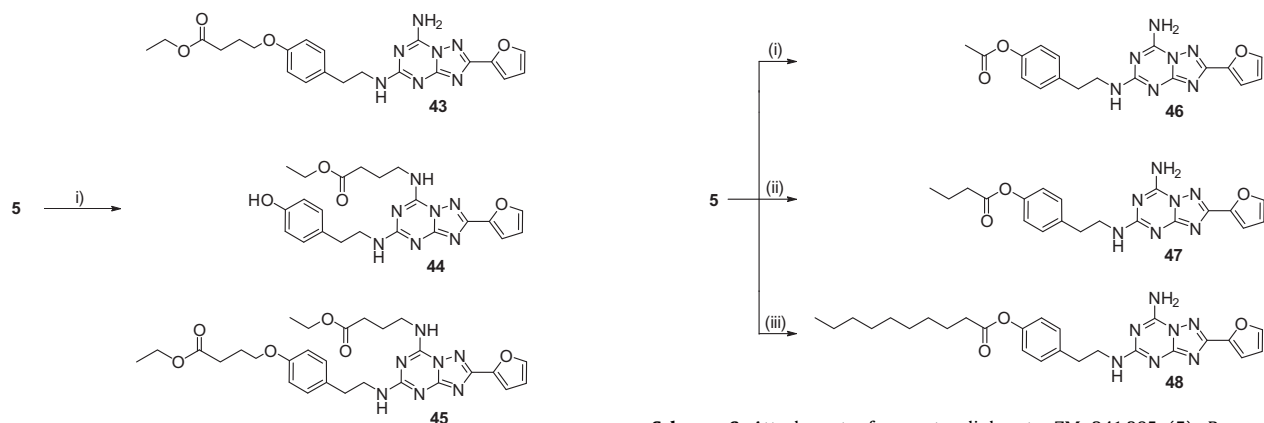


Figure 4. (a) Binding cavity of the A_{2A}R crystal structure (3REY, cyan) with XAC (**4**) bound. A hydrogen bond (black dashes) was observed between the ligand and Asn253. (b) Binding cavity of the A_{2A}R crystal structure (3EML, green) with ZM 241,385 (**5**) bound. Hydrogen bonds were observed between the ligand and Asn253, Glu169, and water molecules. Images were generated using PyMOL software.³⁶



Scheme 4. Attachment of linker groups at the *para*-methoxy position of KW 6002 (**2**). Reagents and conditions: (i) Ac₂O, DMAP, pyridine, 0 °C, 1 h, 79%; (ii) SOCl₂, toluene, 75 °C, 2 h, 96%; (iii) **10**, pyridine, DCM, rt, 16 h, 66%; (iv) HMDS, cat. (NH₄)₂SO₄, MeCN, 160 °C, microwave, 5 h, 95%; LiHMDS, MeI, DMF, 0 °C, 2 h, 67%; (v) LiHMDS, MeI, DMF, 0 °C, 2 h, 67%; (vi) ethyl 4-bromobutyrate, K₂CO₃, NaI, acetone, reflux, 3 d, 57%; (vii) 1 M NaOH, MeOH, 60 °C, 2 h, 88%; (viii) methyl 6-aminohexanoate or methyl 12-aminododecanoate, BOP, DIPEA, DCM, rt, 2 h, 31% (**41**), 37% (**42**).

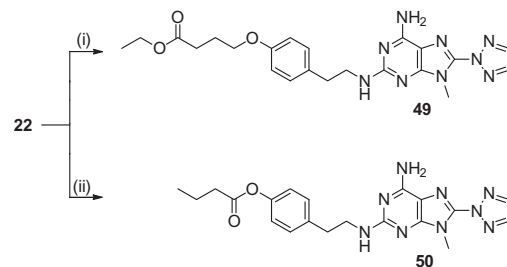


Scheme 5. Attachment of functionality to ZM 241,385 (**5**) using an ether linkage. Reagents and conditions: (i) ethyl 4-bromobutyrate, K₂CO₃, acetone, 50 °C, 46 h, 5% (**43**), 6% (**44**) and 13% (**45**).

Scheme 6. Attachment of an ester linker to ZM 241,385 (**5**). Reagents and conditions: (i) acetyl chloride, TFA, DCM, rt, 44 h, 89%; (ii) butyric anhydride, TFA, DCM, rt, 4 h, 92%; (iii) decanoyl chloride, TFA, DCM, rt, 4 h, 74%.

of the synthesized A_{2A}R antagonists (**2**, **5** and **19–23**) showed that the compounds based on the triazolotriazine scaffold (**5**, **19** and **20**) exhibited the greatest potency. Equal potency was observed between compound **5** (42 nM) and the unsubstituted phenethoxy derivative **20** (41 nM). The substitution of the phenolic oxygen with a bromine atom, however, lead to a four-fold decrease in activity for compound **19**, possibly due to the larger bromine atom and its reduced capacity to act as a hydrogen bond acceptor. The novel hybrid molecules **21–23** showed respectable pIC₅₀ values, but were up to two orders of magnitude less active than the literature compound ZM 241,385 (**5**). A preference for the furan system over the triazole moiety was observed within the hybrid series **21–23**, whereby **21** exhibited significantly greater activity than **22** and **23** (*p* value < 0.05).

Compound **28**, which does not contain a furan ring or triazole moiety, did not show any detectable activity at the A_{2A}R. This



Scheme 7. Attachment of an ester and ether linker to triazole-hybrid (**22**). Reagents and conditions: (i) ethyl 4-bromobutyrate, K₂CO₃, NaI, acetone, reflux, 66 h, 26%; (ii) butyric anhydride, TFA, DCM, rt, 4 h, 92%.

finding is not surprising given that literature postulates the furan ring is essential for the activity of ZM 241,385 (**5**) and structurally related compounds.³⁷

Table 1
Inhibitory potency of synthesized A_{2A}R ligands and monovalent variants using the LANCE™ cAMP assay

Entry	pIC ₅₀ ^a	IC ₅₀ (nM)	Entry	pIC ₅₀ ^a	IC ₅₀ (nM)
2	5.28 ± 0.19	5250	41	4.96 ± 0.04	>10,000
5	7.38 ± 0.06	42	42	<4	>100,000
19	6.74 ± 0.15	182	43	7.30 ± 0.01	50
20	7.39 ± 0.12	41	44	4.59 ± 0.12	>10,000
21	5.58 ± 0.05	2630	45	<4	>100,000
22	5.01 ± 0.01	9770	46	7.41 ± 0.04	39
23	4.26 ± 0.06	>10,000	47	7.53 ± 0.01	30
28	<4	>100,000	48	6.74 ± 0.06	182
38	4.92 ± 0.04	>10,000	49	5.04 ± 0.11	9120
39	5.36 ± 0.16	4370	50	5.01 ± 0.04	9770

^a Data represent the mean ± SEM of two separate experiments performed in duplicate. The pIC₅₀ values of the A_{2A}R antagonists were determined at the EC₅₀ of NECA (500 nM). The EC₅₀ of NECA was determined as 162 nM in the same assay.

KW 6002 (**2**) showed lower antagonism than expected, given its high potency binding results reported in the literature.³⁸ Nonetheless, slight modification of the *para*-methoxy of KW 6002 (**2**) were relatively well tolerated, indicated by the similar activity of compounds **38** and **39** to the parent compound **2**. Extending further with longer chain linkers (compounds **41** and **42**) resulted in diminished potency in a length-dependent manner.

Compounds **43–45** showed consistent potency in support of our hypothesis that the phenolic oxygen is pointing out of the receptor pocket and is therefore the most optimal position for linker attachment. The O-alkylated compound **43** exhibited comparable activity to ZM 241,385 (**5**) whereas the N-alkylated compound **44** was virtually inactive. Not surprisingly, the doubly alkylated compound **45** did not show any detectable activity.

The effect of elongation of the linker at the phenolic oxygen (from **2** to 10 carbon atoms) was investigated with compounds **46–48**. The pIC₅₀ values were mostly maintained compared to the parent compound **5**, although a four fold decrease in activity was observed for compound **48**.

Finally, given the structural similarity of hybrid molecules **21–23** to ZM 241,385 (**5**), it was expected that extension of linkers from the phenolic oxygen would be equally well tolerated from both scaffolds. This was confirmed with the O-linked triazole-hybrids **49** and **50**, which maintained an activity comparable to that of the parent compound **22**, irrespective of linker type used.

To correlate the biological results of the aforementioned compounds to their potential binding mode, molecular modeling was undertaken using published crystal structures of the A_{2A}R. The KW 6002-based compounds, **38–42**, were docked^{39,40} into the thermostabilized A_{2A}R, which was complexed with XAC (**4**) in the crystal structure (3REY, cyan).²⁷ This model was chosen due to the structural similarities between KW 6002 (**2**) and XAC (**4**), most notably the common *N,N*-diethylxanthine unit. To validate the method, XAC (**4**) was redocked into the binding cavity (3REY, cyan), producing a binding mode for the xanthine unit similar to the crystal structure (rmsd of 1.17 Å⁴¹), as seen in Figure 5a. However, the rmsd for the entire molecule dropped (4.07 Å) due to a different orientation of the (2-aminoethyl)acetamido portion caused by additional hydrogen bonding to Glu169 in the docked pose.

Using this receptor model, compounds **38–42** displayed a similar binding site orientation of the xanthine portion, as exemplified by docked poses of **38** (Fig. 5b) and **39** (Fig. 5c). This orientation allowed the extension of linkers towards extracellular space. The length of the linker did not have a significant impact on the binding mode of compounds **38–42**.

The docking of compounds **5**, **19–23** and **43–50** was based on the crystal structure of the T4-lysozyme stabilized A_{2A}R in complex with ZM 241,385 (**5**) (3EML, green).³ To validate the method, ZM 241,385 (**5**) was redocked into the crystal structure and gave a

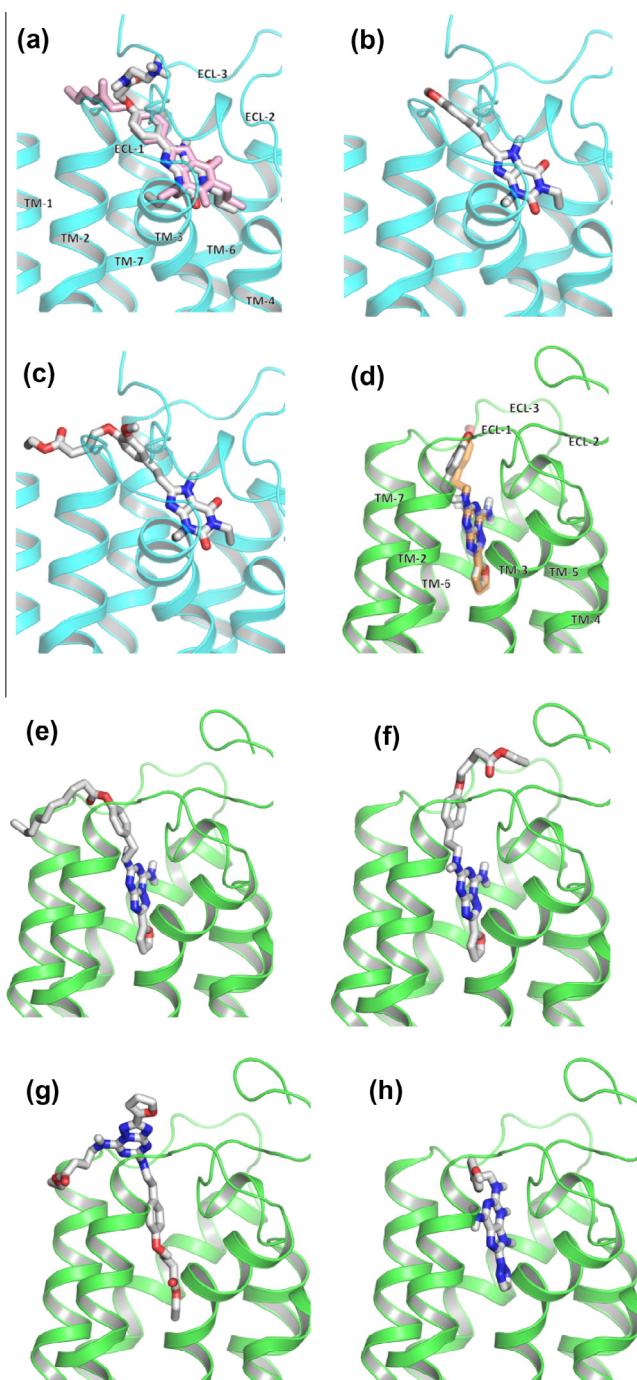


Figure 5. Representation of the A_{2A}R receptor crystal structure (3REY, cyan; 3EML, green) with ligands docked in the binding cavity. Docked ligands: carbon, gray; Nitrogen, blue; oxygen, red. (a) Overlay of docked XAC (**4**) with bound crystal structure ligand (fuchsia); (b) compound **38**; (c) compound **39**; (d) overlay of docked ZM 241,385 (**5**) with bound crystal structure ligand (orange); (e) compound **48**; (f) compound **43**; (g) compound **45**; (h) compound **22**. Images were generated using PyMOL software.³⁶

comparable binding mode with acceptable rmsd for the entire molecule of 1.67 Å,⁴¹ (Fig. 5d). Compounds **19** and **20** showed the same binding mode as ZM 241,385 (**5**).

Next, we explored the effect on binding mode of alkylation at various positions of ZM 241,385 (**5**). Linker-attachments on the terminal phenolic group in compounds **43**, **46–48** had minimal effect on docked poses and confirmed the benefit of attaching alkyl groups at this position to extend toward the extracellular space. The length and nature of the linker attached from this position

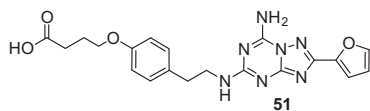


Figure 6. Proposed structure of the first triazolotriazine carboxylic acid congener (TCAC) **51**.

caused little effect on the binding mode of the scaffold (illustrated in Fig. 5e and 5f). The orientation of the alkyl group allows extension towards the extracellular space, thus minimizing interference with key binding site interactions. The alkylation of the amino group to yield **44** and **45** resulted in a flipped binding mode (Fig. 5g). This finding may explain the observed reduction in antagonistic activity of these compounds compared to ZM 241,385 (**5**), as the crucial binding interactions are lost.

The hybrid molecules **21–23** and linker-extended analogs **49–50**, all based on a purine scaffold, generally gave docked poses similar to ZM 241,385 (**5**). These compounds, however, were unable to penetrate as deep into the binding pocket as exemplified in Figure 5h. This phenomenon, in addition to the missing nitrogen atom at position 5 and introduced N-methyl group at position 7, potentially explains the lower IC_{50} values observed for the hybrid molecules.

In conclusion, the phenolic oxygen of ZM 241,385 (**5**) has been shown to be a suitable position to attach linkers. In addition, compound **43** has emerged to be the ideal structure for further studies of the $A_{2A}R$. From the aforementioned biological data, compound **43** was identified as a high affinity analog of ZM 241,385 (**5**). Its terminal ester group allows for facile functionalization and chemical elaboration. This structural feature is in accordance with the concept of a 'functionalized congener',²¹ a molecule that comprises a chemical functional group (e.g. amine or carboxylic acid) that is suitably linked to a pharmacophore. We envisage the hydrolysis of **43** to afford compound **51** (Fig. 6), a functionalized congener, revealing a carboxylic acid functionality that can be utilized to synthesize pharmacological conjugates such as bivalent ligands, bitopic ligands and biomarkers. In relation to the molecule XAC (**4**), a xanthine-based versatile congener widely used to study adenosine receptorology, compound **51** has emerged as a triazolotriazine-based equivalent (Triazolotriazine Carboxylic Acid Congener (TCAC)) that warrants further investigation.

In summary, the investigation of our series of $A_{2A}R$ ligands, based on the literature compounds KW 6002 (**2**) and ZM 241,385 (**5**), revealed that (i) compounds **46**, **20**, **5** and **43** (with IC_{50} values of 39, 41, 42 and 50 nM, respectively) are equipotent to the literature compound ZM 241,385 (**5**) (IC_{50} = 42 nM) (Table 1); (ii) the attachment of an ester or ether linker to the phenolic oxygen of ZM 241,385 (**5**) was well tolerated; (iii) linkers up to 10 carbon atoms in length were well tolerated when incorporated into ZM 241,385 (**5**) but less so with the KW 6002 (**2**) scaffold; (iv) identification of molecule **51** as a novel TCAC with scope to further explore the $A_{2A}R$ and associated extracellular space. The biological results, in conjunction with molecular modeling, supported our working hypothesis: the phenolic oxygen is a highly suitable position for the attachment of functionalized linkers to extend towards extracellular space from the $A_{2A}R$.

Acknowledgments

M.J. is a recipient of the Australian Postgraduate Award Industry (APAI). J.S. is a recipient of the Australian Postgraduate Award (APA). Thank you to Phoebe Lei and Qianqian Wu (GSK R&D, China) for performing the $A_{2A}R$ functional assay. Thank you to Dr Jason Dang (Monash University) for helping obtain NMR spectral data, HRMS and HPLC chromatograms.

Supplementary data

Supplementary data associated with this article can be found, in the online version, at <http://dx.doi.org/10.1016/j.bmcl.2013.03.070>.

References

- Fredholm, B. B.; Chen, J.-F.; Masino, S. A.; Vaugeois, J.-M. *Annu. Rev. Pharmacol. Toxicol.* **2005**, *45*, 385.
- Fredholm, B. B.; Ijzerman, A. P.; Jacobson, K. A.; Klotz, K.-N.; Linden, J. *Pharmacol. Rev.* **2001**, *53*, 527.
- Jaakola, V.-P.; Griffith, M. T.; Hanson, M. A.; Cherezov, V.; Chien, E. Y. T.; Lane, J. R.; Ijzerman, A. P.; Stevens, R. C. *Science* **2008**, *322*, 1211.
- Ross, G. W.; Abbott, R. D.; Petrovitch, H.; Morens, D. M.; Grandinetti, A.; Tung, K.-H.; Tanner, C. M.; Masaki, K. H.; Blanchette, P. L.; Curb, J. D.; Popper, J. S.; White, L. R. *J. Am. Med. Assoc. (JAMA)* **2000**, *283*, 2674.
- Chen, J. F.; Xu, K.; Petzer, J. P.; Staal, R.; Beilstein, M.; Sonsalla, P. K.; Castagnoli, K.; Castagnoli, N., Jr; Schwarzschild, M. A. *J. Neurosci.* **2001**, *21*, RC143 (1–6).
- Bibbiani, F.; Oh, J. D.; Petzer, J. P.; Castagnoli, N.; Chen, J. F.; Schwarzschild, M. A.; Chase, T. N. *Exp. Neurol.* **2003**, *184*, 285.
- Tronci, E.; Simola, N.; Borsini, F.; Schintu, N.; Frau, L.; Carminati, P.; Morelli, M. *Eur. J. Pharmacol.* **2007**, *566*, 94.
- LeWitt, P. A.; Guttman, M.; Tetrad, J. W.; Tuite, P. J.; Mori, A.; Chaikin, P.; Sussman, N. M. *Ann. Neurol.* **2008**, *63*, 295.
- Pinna, A. *Expert Opin. Invest. Drugs* **2009**, *18*, 1619.
- Postuma, R. B.; Lang, A. E.; Munhoz, R. P.; Charland, K.; Pelletier, A.; Moscovich, M.; Filla, L.; Zanatta, D.; Rios, R. S.; Altman, R.; Chuang, R.; Shah, B. *Neurology* **2012**, *79*, 651.
- Müller, C. E.; Jacobson, K. A. *Biochim. Biophys. Acta* **2011**, *1808*, 1290.
- Kecskés, A.; Tosh, D. K.; Wei, Q.; Gao, Z.-G.; Jacobson, K. A. *Bioconjugate Chem.* **2011**, *22*, 1115.
- Shonberg, J.; Scammells, P. J.; Capuano, B. *ChemMedChem* **2011**, *6*, 963.
- Morphy, R.; Kay, C.; Rankovic, Z. *Drug Discovery Today* **2004**, *9*, 641.
- Valant, C.; Sexton, P. M.; Christopoulos, A. *Mol. Interv.* **2009**, *9*, 125.
- Berque-Bestel, I.; Lezoulac'h, F.; Jockers, R. *Curr. Drug Disc. Technol.* **2008**, *5*, 312.
- Portoghesi, P. S.; Larson, D. L.; Yim, C. B.; Sayre, L. M.; Ronsisvalle, G.; Lipkowski, A. W.; Takemori, A. E.; Rice, K. C.; Tam, S. W. *J. Med. Chem.* **1985**, *28*, 1140.
- McRobb, F. M.; Crosby, I. T.; Yuriev, E.; Lane, J. R.; Capuano, B. *J. Med. Chem.* **2012**, *55*, 1622.
- Vernall, A. J.; Stoddart, L. A.; Briddon, S. J.; Hill, S. J.; Kellam, B. *J. Med. Chem.* **2012**, *55*, 1771.
- Baker, J. G.; Middleton, R.; Adams, L.; May, L. T.; Briddon, S. J.; Kellam, B.; Hill, S. *J. Br. J. Pharmacol.* **2010**, *159*, 772.
- Jacobson, K. A.; Ukena, D.; Padgett, W.; Kirk, K. L.; Daly, J. W. *Biochem. Pharmacol.* **1987**, *36*, 1697.
- Jacobson, K. A.; Daly, J. W. *Nucleosides Nucleotides* **1991**, *10*, 1029.
- Hockemeyer, J.; Burbiel, J. C.; Müller, C. E. *J. Org. Chem.* **2004**, *69*, 3308.
- Burbiel, J. C.; Hockemeyer, J.; Müller, C. E. *J. Org. Chem.* **2006**, *2*, 20.
- Caulkett, P.W.R.; Jones, G.; Collis, M.G.; Poucher, S.M. EP 459702, 1991.
- Caulkett, P. W. R.; Jones, G.; McPartlin, M.; Renshaw, N. D.; Stewart, S. K.; Wright, B. *J. Chem. Soc., Perkin Trans. 1* **1995**, *7*, 801.
- Doré, A. S.; Robertson, N.; Errey, J. C.; Ng, I.; Hollenstein, K.; Tehan, B.; Hurrell, E.; Bennett, K.; Congreve, M.; Magnani, F.; Tate, C. G.; Weir, M.; Marshall, F. H. *Structure* **2011**, *19*, 1283.
- Jörg, M.; Agostino, M.; Yuriev, E.; Mak, F.; Miller, N.; White, J.; Scammells, P.; Capuano, B. *Struct. Chem.* **2012**. <http://dx.doi.org/10.1007/s11224-012-0151-7>, published online.
- Srivastava, R. P.; Kumar, V. V.; Bhatia, S.; Sharma, S. *Indian J. Chem., Sect. B* **1995**, *34B*, 209.
- Dolzhenko, A. V.; Pastorin, G.; Dolzhenko, A. V.; Chui, W. K. *Tetrahedron* **2009**, *50*, 2124.
- Gorgio, T.; Giovann, P.; Patrizia, M.; Maria Assunta Di, C.; Grazia, G.; Fabrizio, G.; Luca, G. WO03011864, 2003.
- Janssen, P.A.J.; Lewi, P.J.; De Jonge, M.R.; Koymans, L.M.H.; Daeyaert, F.F.D.; Heeres, J.; Vinkers, H.M.; Leenders, R.G.G.; Vandenput, D.A.L. WO 2005028479, 2005.
- Foitzik, R. C.; Devine, S. M.; Hausler, N. E.; Scammells, P. *J. Tetrahedron* **2009**, *65*, 8851.
- Maruyama, T.; Kozai, S.; Sasaki, F. *Nucleosides, Nucleotides Nucleic Acids* **2000**, *19*, 1193.
- Bartocchini, F.; Cabri, W.; Celona, D.; Minetti, P.; Piersanti, G.; Tarzia, G. *J. Org. Chem.* **2010**, *75*, 5398.
- Schrödinger, L.L.C. The PyMOL Graphics System, version 1.5.0.4; New York, NY, 2010.
- Alanine, A.; Anselm, L.; Steward, L.; Thomi, S.; Vifian, W.; Groaning, M. D. *Bioorg. Med. Chem. Lett.* **2004**, *14*, 817.
- Chen, J. F.; Xu, K.; Petzer, J. P.; Staal, R.; Xu, Y. H.; Beilstein, M.; Sonsalla, P. K.; Castagnoli, K.; Castagnoli, N., Jr; Schwarzschild, M. A. *J. Neurosci.* **2001**, *21*:RC143 (1–6).
- Friesner, R. A.; Banks, J. L.; Murphy, R. B.; Halgren, T. A.; Klicic, J. J.; Mainz, D. T.; Repasky, M. P.; Knoll, E. H.; Shelley, M.; Perry, J. K.; Shaw, D. E.; Francis, P.; Shenkin, P. S. *J. Med. Chem.* **2004**, *47*, 1739.
- McRobb, F. M.; Capuano, B.; Crosby, I. T.; Chalmers, D. K.; Yuriev, E. *J. Chem. Inf. Model.* **2010**, *50*, 626.
- Yuriev, E.; Agostino, M.; Ramsland, P. A. *J. Mol. Recognit.* **2011**, *24*, 149.